

*Proceedings of the Korean Nuclear Society Autumn Meeting*  
*Seoul, Korea, October 1998*

**Dynamic Pressure Assessment for the Steam Explosion in a PWR Cavity using TEXAS**

Moonkyu Hwang and Soo-Yong Park

Korea Atomic Energy Research Institute  
150 Dukjin-dong, Yusong-ku  
Taejon, Korea 305-353

**Abstract**

One-dimensional three-phase code TEXAS is used for the assessment of dynamic pressure load induced by steam explosion phenomena which might occur in a PWR cavity structure during severe accident scenario. To overcome the limitation imposed by the one-dimensionality of TEXAS code, premixing phase of the steam explosion is simulated by IFCI code which has a two-dimensional capability. The code-simulated results show that the pressure behavior generally conforms to the typical experimental observation and also reveal the importance of trigger time. The sensitivity study shows that the magnitude of the pulse is lowered by about 35 % when the cross sectional area is doubled from 0.2 m<sup>2</sup> to 0.4 m<sup>2</sup>. The increased premixing void fraction for the delayed triggering time from 1 second to 2 second suggests minimal pressure generation because of water voiding effect.

**1. Introduction**

When a cold liquid is brought into contact with a molten material with a temperature significantly higher than the liquid boiling point, an explosive interaction due to sudden fragmentation of the melt and rapid evaporation of the liquid may take place. This phenomenon is referred to as a steam explosion or vapor explosion.

Depending upon the amount of the melt and the liquid involved, the mechanical energy released during a vapor explosion can be large enough to cause serious destruction. Such incidents were observed in the aluminum industry where molten aluminum was handled near water, and resulted in not only property damage, but also fatalities in some cases.

Steam explosions have been of concern also in the nuclear industry. In hypothetical severe accidents which involve fuel melt down, subsequent interactions between the molten fuel and coolant may cause steam explosion. This process has been studied by many investigators in an effort to assess the likelihood of containment failure which could lead to large scale release of radioactive materials to the environment.

Large-scale vapor explosions initiating from melt-on-coolant contact are known to go through four distinct phases; namely, coarse mixing, triggering, propagation, and expansion. The four phases of the process are briefly described below.

**Coarse Mixing:** As the hot melt falls into the liquid coolant, it breaks up into globules nearly 1cm in diameter in the case of molten corium and water. Film boiling occurs at the surface of each hot globule without significant heat transfer from the melt to the liquid coolant. In this phase, the melt drops, vapor film, vapor bubbles, and liquid coolant remain in a metastable condition. The process can last about one second.

**Triggering:** The metastable stage of coarse mixing can be transformed to liquid-liquid contact between the melt and coolant by disturbance of the vapor blanket around the melt. The process can happen

spontaneously, usually next to solid surfaces in a confined geometry, or can be initiated by a pressure pulse which locally destabilizes the film layer between the melt and coolant. The triggering phase initiates efficient heat transfer between the liquid coolant and the molten material.

Propagation: Following the triggering phase, high pressure coolant vapor is generated, and a disturbance pulse travels through the whole coarse mixing region leading to direct contact between the molten material and liquid coolant. In this stage, part of the molten liquid undergoes fine fragmentation producing very large melt-coolant interfacial area, which in turn leads to higher heat transfer between the two.

Expansion: The high pressure vapor generated in the propagation phase expands against the surrounding material. Part of the thermal energy transferred from the molten material to the coolant is transformed into mechanical energy during this phase, and may result in the destruction of the surrounding structures.

This study presents the methodology and results of the dynamic pressure load calculation for typical PWR containment cavity. The main tool used for the dynamic pressure estimation was TEXAS code developed at University of Wisconsin at Madison, with the aid of IFCI code from Sandia National Laboratories. The ex-vessel energetic fuel-coolant interaction or steam explosion under consideration is postulated to follow the core meltdown and eventual melt release to the pre-flooded cavity.

## 2. TEXAS and IFCI Models for Fuel/Coolant Interaction

TEXAS [1,2,3] is model based on a one-dimensional hydrodynamics code developed at Sandia National Laboratories and modified for fuel-coolant interactions. The model solves the 1-D, three-field equations describing the fuel, coolant vapor and liquid. Two fields represent the coolant as a separate liquid and vapor in an Eulerian control volume, while one field models the fuel as discrete material volumes (or ‘master particles’) in a Lagrangian formulation within this Eulerian region. In this model the governing conservation equations for each phase (i.e., liquid and vapor coolant and fuel particles) are written separately allowing for mechanical and thermal nonequilibrium to exist between the phases. The effects of condensation, evaporation, and interfacial momentum transport are included as source and sink terms in the balance equations. The two key constitutive relations involve hydrodynamic fragmentation of the fuel ‘master particles’ based on Rayleigh-Taylor instabilities during the mixing phase, and thermal fragmentation of the fuel and rapid quench during the explosion phase.

In the case of fuel mixing, it is postulated that this model of instability is caused by the relative velocity between the incoming fuel (as a jet or as discrete ‘blobs’) and the coolant and is dominant compared to other instabilities (i.e. Kelvin-Helmholtz or Boundary layer stripping) because of the effects of vapor film boiling which may suppress these other processes. A complete theoretical model for Rayleigh-Taylor breakup was initially formulated and was then implemented in TEXAS as a simplified linear correlation of the theoretical model. The Lagrangian particle size at a new time (n+1) using the field variables at the old time level (n) without any reference to the history of the particle is given by the expression

$$D^{n+1} = D^n (1 - C_0 \Delta T^+ We^{C_3}) \quad (1)$$

where  $\Delta T^+$  is the dimensionless time step [ $v \Delta t / D^* \epsilon$ ],  $We$  is the Weber number evaluated at the relative velocity and  $\epsilon$  is the square root of the density ratio of the continuous-dispersed phases at the old time level, and the constants,  $C$ , are empirically determined constants from the complete theoretical model.

The thermal fragmentation rate model for the fuel during the explosion phase is a semi-empirical formulation based on the concept of vapor film boiling collapse and coolant jet impingement on the fuel surface. The fuel mass fragmentation rate for a particular master particle is given by a expression

$$m_{fr} = C r_f \rho D_f^2 N_f [(P - P_\infty) / r_c]^{1/2} F \quad (2)$$

where  $N$  is the number of discrete fuel particles,  $f$ , in a ‘master particle’,  $D_f$  is the fuel diameter,  $P$  and  $P_\infty$  are the local fluid pressure and the initial ambient pressure, respectively. The constant,  $C$ , is the model constant estimated by past theoretical work of Kim [4] and empirically determined by analysis of the KROTOS test (0.001 to 0.002). The factor,  $F$ , varies from 1 to 0 at the time when the fragmentation time reached. This fragmentation time was empirically found to vary from 0.5 to 2.0 msec for good agreement with the KROTOS tests (alumina and tin simulants for the fuel). The rate of coolant vaporization from the quenching of this fragmented fuel during the explosion is found by considering the fragmented fuel to be a heat source to the coolant vapor-liquid interface and the rate of vapor formation is determined by the difference in this heat difference from the vapor to the bulk liquid coolant.

The explosion is assumed to be triggered by the postulated existence of a high pressure volume at the base of the water pool. This pressure could be due to a local fuel-coolant interaction or impact of some solid object upon the floor ( $\sim 1$ MPa), and transmits its pressure pulse to the mixture as the volume (a few cc) expands.

The purpose of the IFCI code is to predict steam generation rate, melt fragmentation and dispersion, shock wave generation and propagation, and, system loading for explosive and non-explosive FCIs. IFCI models the four stages of a steam explosion: 1) coarse fragmentation and mixing of molten material with water, 2) triggering, 3) propagation and fine fragmentation, and 4) expansion of the melt water system.

The equation set used in IFCI is a four field, two-dimensional, cylindrical geometry version of a set commonly used in multifield computational hydrodynamics and originally derived by Ishii [5]. A field in the context of multifield hydrodynamics is represented by separate mass continuity, momentum, energy equations for each type and phase of material in the interaction. These three equations are solved for each field. Mass, energy, and momentum transfer between fields are represented by coupling terms in the field equations for which constitutive relations must be provided. The field equations, along with constitutive laws, equations of state are solved by use of the SETS method developed by Mahaffy [6].

In IFCI, a melt drop is described by an Eulerian melt field interacting with the water and steam fields, which are also Eulerian. The fuel characteristic size may either be smaller than a finite difference mesh cell (i.e., subgrid size) or extend over more than one cell. In the subgrid case, the fuel melt exists as discrete drops, which IFCI treats with models for primary breakup and surface entrainment. The primary breakup and surface entrainment models provide source term for a continuity equation for melt volumetric surface area. In case the melt extent is greater than the finite difference grid, surface area generation takes place as the melt geometry distorts due to hydrodynamic motion on the grid. IFCI uses a surface area tracking model/algorithm to handle this case.

The idea of dynamic fragmentation model which calculates the characteristic melt diameter as a function of instantaneous hydrodynamic conditions was first proposed by Camp (Young [7]). A model using this idea was later incorporated into a version of the TEXAS one-dimensional FCI code. The fragmentation model in IFCI is a version of a dynamic fragmentation model developed by Pilch [8] based on Rayleigh-Taylor instability theory and the existing body of gas-liquid and liquid-liquid drop breakup data.

The basic Pilch model describes primary breakup of a drop via penetration of the drop by Rayleigh-Taylor waves, and is expressed as

$$\frac{dD}{dt} = \frac{(1 - N^{-1/3})}{T^+} |V_r| e^{0.5} \quad (3)$$

This formulation was developed from the empirical observation that, in high Weber number drop breakup experiments, the drop experiences primary breakup into 3-5 primary fragments in a dimensionless time  $T^+$  between 1 and 1.25. While primary breakup is occurring, smaller fingers continuously develop and break off, forming a cloud of droplets. This effect is included in IFCI via surface entrainment model

$$\frac{dS}{dt} = C_0 C_f^{0.75} \frac{1}{D} We^{0.25} |V_r| e^{0.5} \quad (4)$$

where  $dS/dt$  is the surface entrainment rate per unit melt area, and  $C_0$  is a constant 0.089.

### 3. Initial Conditions for Ex-vessel Steam Explosion

For the assessment of ex-vessel steam explosion dynamic pressure load, a representative initial condition is necessary. However, the estimation of the mass of molten corium in ex-vessel steam explosion and other physical parameters needed for detailed analysis involves a quite degree of uncertainties. For the current study, only the bounding situation which is practically expected is considered, and the ICI tube ejection was chosen as a typical vessel failure mechanism. The initial diameter of ICI tube was chosen as 7.5cm and during 1second it ablates according to  $r_0+Bt$ . With the values of 0.05m and 0.0375m for B and  $r_0$ , respectively, the final hole diameter after 1second of ablation becomes 17.5cm.

Since TEXAS does not allow varying initial melt diameter, it is necessary to assign a constant inlet melt diameter for the code calculation. The diameter of the inlet melt was assumed to be 20cm throughout the mixing process rather than varying from initial hole size of 7.5 cm to the final ablated hole size. This conservative value would provide more melt mass to be involved in EVSE than in real situation. The initial melt velocity was obtained from

$$U_0 = \left( 2 g \Delta z + \frac{2\Delta P}{\rho} \right)^{1/2} \quad (5)$$

When the pressure difference does not exist, and with of assumed melt height in the lower plenum of 1.5 meter, the initial melt discharge velocity is 5.4 meter /sec. The mass of melt discharged during 1 second is therefore,

$$\begin{aligned} M_{total} &= (Hole Area) \times (Melt Velocity) \times (Melt Density) \times (1 sec) \\ &= \rho (0.1m)^2 \times 5.4 m / sec \times 8800 kg / m^3 \times 1 sec \\ &\cong 1500 kg \end{aligned}$$

where melt density of 8800Kg/m<sup>3</sup> was used as a typical value. The melt temperature in the present analysis was taken as 2900K. This value provide the superheat of 100K when melting temperature is taken as a typical value of 2800K. The cavity pressure was chosen to be 0.2 MPa, and the cavity water temperature of 353 K and gas temperature of 393K were used.

### 4. Results and Discussions

As described earlier in section 2, TEXAS code in its current version has a restriction of 1-D simulation. The radial behavior, therefore, is completely neglected during the coarse fragmentation and melt/water mixing. This is true for the propagation and expansion stages as well. During the premixing phase, however, the radial expansion of melt and mixing behavior is important since it determines the melt/water mass ratio at the moment of triggering.

In this calculation, IFCI from Sandia National Laboratories was used to determine the extent of radial dispersion of melt after water inlet. The cross sectional area is then used for the calculation using TEXAS. That is, IFCI is only used to assess the cross sectional area, and TEXAS calculation is again made for the whole stage of steam explosion based on the cross section area obtained from IFCI calculation. With the initial conditions described in section 3, the cross sectional area of 0.2 m<sup>2</sup> was obtained by IFCI calculation.

The whole stage for ex-vessel steam explosion starting from the premixing phase was simulated using TEXAS, for the cross sectional area of 0.2 m<sup>2</sup>, 0.3 m<sup>2</sup>, and 0.4 m<sup>2</sup> for comparison. For each calculation, the total of 40 axial meshes were used. Initially lower 22 meshes were assigned for cavity

water and remaining 18 meshes were used for the air zone. For a typical PWR cavity, the water height was assumed to be 5.5 meter at the time of vessel failure. The mesh size was therefore 0.25m.

TEXAS handles the triggering time as a input parameter. That is, user defines the time of triggering. The triggering mechanism and it criteria are hardly understood at present time. The triggering time of 1second was used throughout the analysis, except for 2sec as a added calculation for 0.2 m<sup>2</sup> cross sectional area.

Figures from 1 to 10 show the results of simulations for the cross sectional areas of 0.2 m<sup>2</sup>, 0.3 m<sup>2</sup>, and 0.4 m<sup>2</sup>, as noted respectively. The melt discharged during the first 1second was about 1500kg. Fig 1,4, and 7 show corium melt and void volume fraction distributions along the cavity height. As seen from these figures, most part of corium melt stays between 2.0 m and 6.5m from the bottom of the cavity. For the calculations with 0.3 m<sup>2</sup> and 0.4m<sup>2</sup> cross sectional areas, generally lower values of volume fractions are observed in the mixture zone, as expected. This is simply because of larger amount of water involved. One can also see the little more penetration toward the bottom of cavity. Also seen is the water level swell, which is obvious from the void fraction distribution. With lager cross sectional are, the level swell was diminished. The largest melt volume fraction of 0.4 is observed at the height of about 3.2m for cross sectional area of 0.2 m<sup>2</sup>. In cases for the cross sectional areas of 0.3 m<sup>2</sup> and 0.4 m<sup>2</sup>, more of less uniform melt distributions, where they appear, are observed. Generally, one can conclude that the premixing volume distributions of melt and void are very similar for 3 different cross sectional areas, give the triggering time of 1second. The volume fraction distributions for melt and void, however, are quite different when triggering is delayed to 2 second. As seen from figure 10, due to the extended duration of premixing time and resulting thermal interaction, large void fraction close to 1.0 is observed from the height from about 3.5 m to 8 m. The melt is seen to penetrate deeper into below 2m high.

The pressure histories during propagation phases are depicted for node 14 to node 24 in Figures 2, 3, 5, 6, 8, and 9. These pressure pulses are generated from steam explosion triggered at time of 1 second. As seen in these figures, the time scales are those of typical steam explosion situations. The major peaks appear within the time order of about 3 msec after triggering. In figure 2, which is for the case of 0.2 m<sup>2</sup> of cross sectional area, the peak pressure of about 140 MPa is observed at the node 18. Since the node size was 0.25 m, the node for the peak pressure is about 4.4 meter from the bottom of cavity. When the cross sectional area of 0.3 m<sup>2</sup> was used, as seen in figure 4, the peak pressure value was about 125 MPa at the height of around 4 m. The peak value is even lowered to less than 100MPa when the cross sectional area is increased to 0.4 m<sup>2</sup>, as seen from figure 6.

The cross sectional area of 0.2 m<sup>2</sup>, 0.3 m<sup>2</sup> and 0.4 m correspond to discs whose radius are about .25 m, 0.3 m, and 0.36 m, respectively. If the explosion occurs near the axis of the PWR cavity, the pressure pulse will be attenuated as it travels to the cavity wall. At least 2-D analysis using codes such as IFCI would provide more realistic answer for this situation. However, if pressure attenuation in TNT analogy is used, the pressure will be reduced by factor of R<sup>α</sup>, where R is distance in feet and the value of α is taken to be 1.13 [3]. For the typical cavity whose nearest distance from the center is 7 feet. the pressure at the center of cavity will be attenuated by factor of about 9. The peak pressure of 150 MPa, in this calculation, would be then 16 MPa at the nearest cavity wall.

The pressure pulse history with trigger time of 2 sec would have provide quite informative data for comparison. The calculation was, however, not successful because of numerical instability of the code. But as seen in figure 10, the void fraction in the water/gas mixture is quite high where the melt is observed. This fact suggests much lessened pressure pulse, simply because there aren't enough water to be *burned* to steam during propagation stage. Since only small amount of water is present in this region, dynamic pressure generation which would threaten cavity integrity is hardly expected.

## 5. Conclusions

One-dimensional three-phase code TEXAS is used for the assessment of dynamic pressure load induced by steam explosion phenomena which might occur in a PWR cavity structure during severe accident scenario. To overcome the limitation imposed by the one-dimensionality of TEXAS code,

premixing phase of the steam explosion is simulated by IFCI code which has a two-dimensional capability. The sensitivity analysis with respect to cross sectional area showed that the premixing behaviors were generally very similar with each other. The melt and void fraction distributions along the axis of the cavity were nearly same. The general trends of the pressure pulses during the propagation phase were also similar. The magnitude of the pulse, however, was lowered by about 35 % when the cross sectional area was doubled from 0.2 m<sup>2</sup> to 0.4 m<sup>2</sup>. The premixing volume fraction for the delayed triggering time from 1 second to 2 second suggests minimal pressure generation because of water voiding effect.

#### References

1. C.C. Chu, "One-Dimensional Transient Fluid Model for Fuel-Coolant Interaction Analysis," Ph.D. Thesis, University of Wisconsin (1986).
2. J. Tang, "Modelling of the Complete Process of One-Dimensional Vapor Explosions," Ph.D. Thesis, University of Wisconsin (1993).
3. M.F. Young, "The TEXAS Code for Fuel-Coolant Interaction Analysis," Proc. ANS/ENS LMFBR Safety Topical Mtg., Lyon-Ecully, France (1982).
4. B. Kim, "Heat Transfer and Fluid Flow Aspect of Small-Scale Single Droplet Fuel-Coolant Interaction," Ph.D. Thesis, University of Wisconsin, Madison (1985).
5. M. Ishii, "Thermo-Fluid dynamic Theory of Two-Phase Flow", Eyrolles, France (1975)
6. J. H. Mahaffy, "A Stability-Enhancing Two-Step Method for Fluid Flow Calculations," J. Comp. Phys. 46, p329, (1982)
7. M. F. Young, et. al "The FCI Potential of Oxide and Carbide Fuels: Results and the Prompt burst Series at Sandia National Laboratories," Fourth CSNI Specialist Meeting on Fuel-Coolant Interaction in Nuclear Reactor Safety, Bournemouth, UK.(1979)
8. M. Pilch, "Acceleration Induced Fragmentation of Liquid Drops," Ph.D. Thesis," University of Virginia, Charlottesville, VA, (1981)
9. Cole, R. H., "Underwater Explosion," Princeton University Press, Princeton, New Jersey, 1948

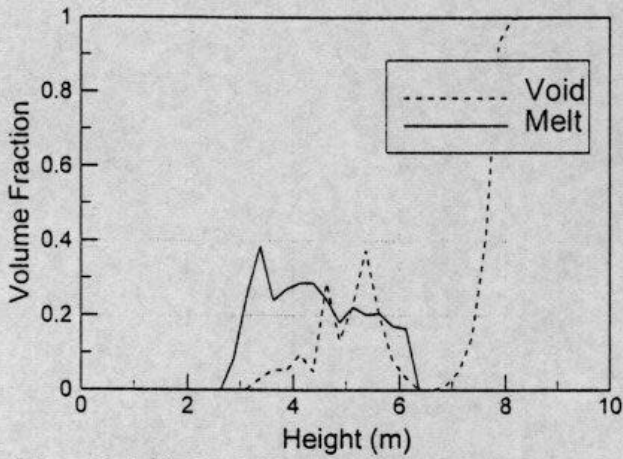


Figure 1. Melt fraction and void fraction in water/gas mixture ( $A=0.2 \text{ m}^2$ , Trigger=1 sec)

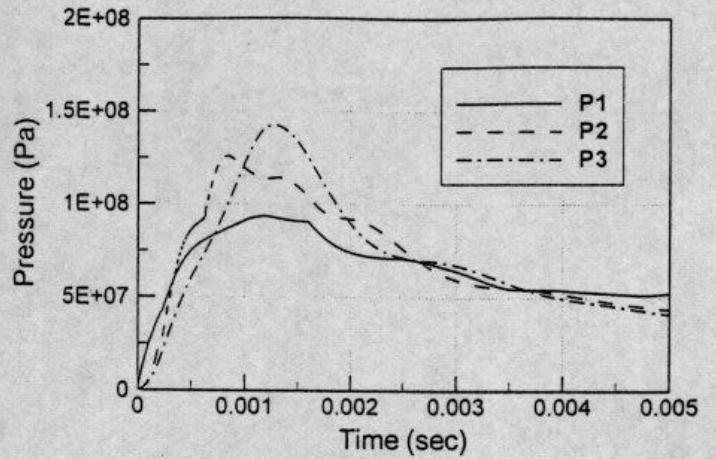


Figure 2. Pressure pulses at node 14, 16, 18 ( $A=0.2 \text{ m}^2$ , Trigger=1 sec)

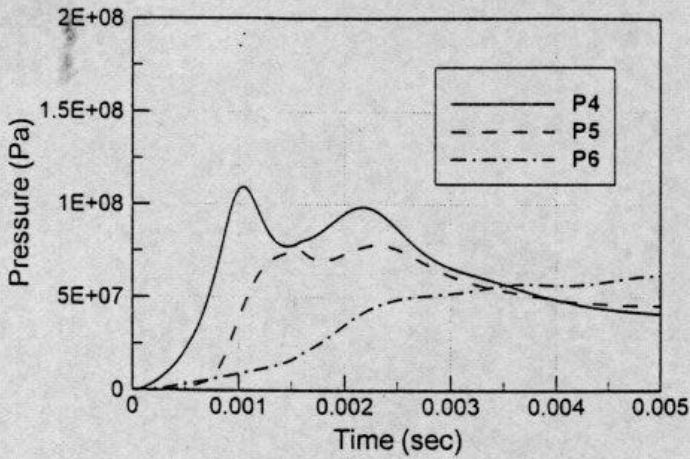


Figure 3. Pressure pulses at node 20, 22, 24 ( $A=0.2 \text{ m}^2$ , Trigger=1 sec)

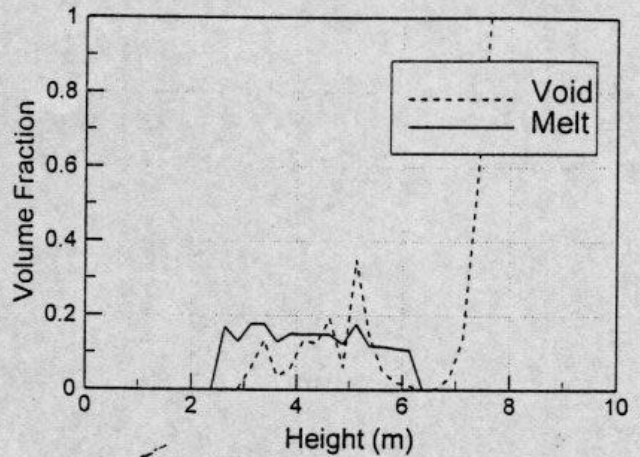


Figure 4. Melt fraction and void fraction in water/gas mixture ( $A=0.2 \text{ m}^2$ , Trigger=1 sec)

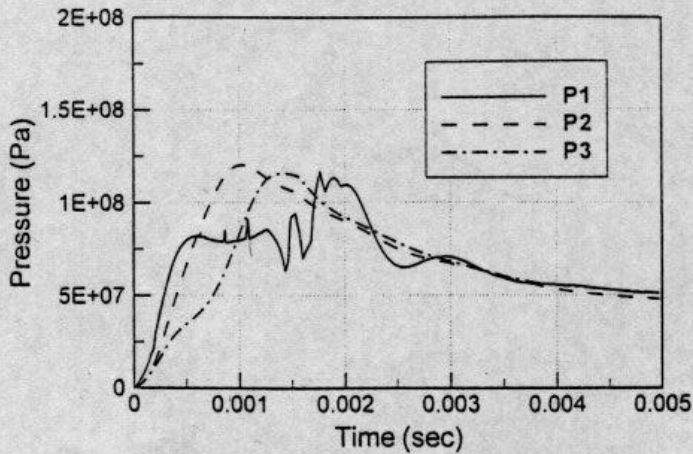


Figure 5. Pressure pulses at node 14, 16, 18 ( $A=0.3 \text{ m}^2$ , Trigger=1 sec)

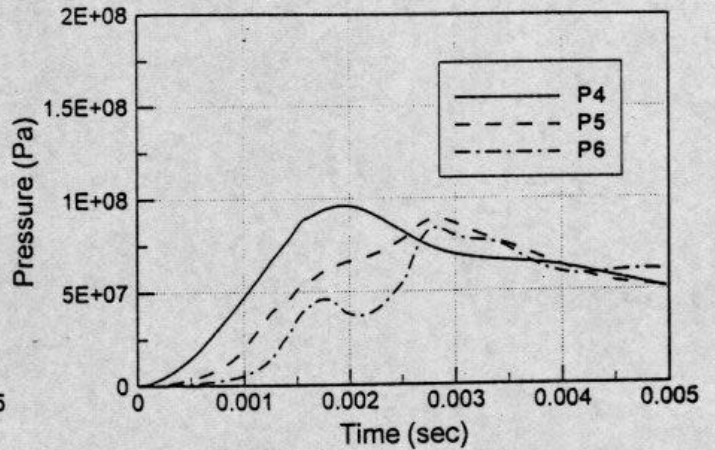


Figure 6. Pressure pulses at node 20, 22, 24 ( $A=0.3 \text{ m}^2$ , Trigger=1 sec)

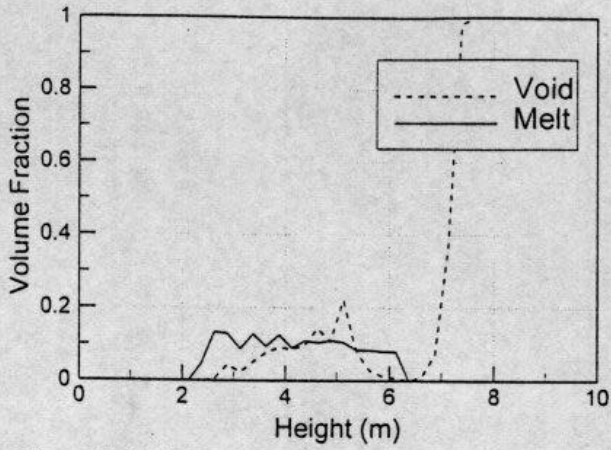


Figure 7. Melt fraction and void fraction in water/gas mixture ( $A=0.2 \text{ m}^2$ , Trigger=1 sec)

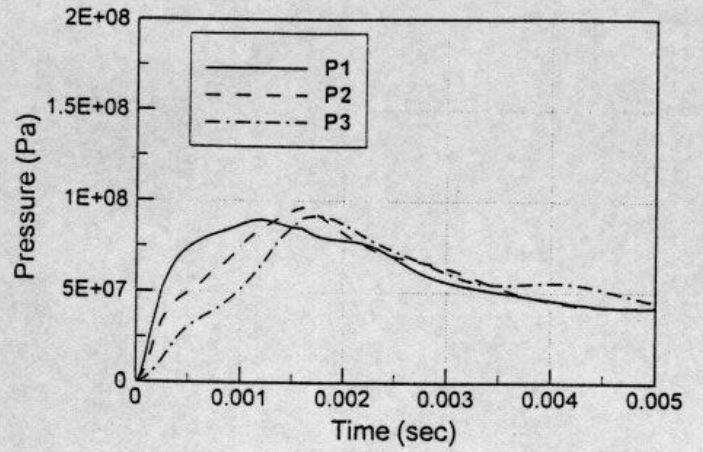


Figure 8. Pressure pulses at node 14, 16, 18 ( $A=0.4 \text{ m}^2$ , Trigger=1 sec)

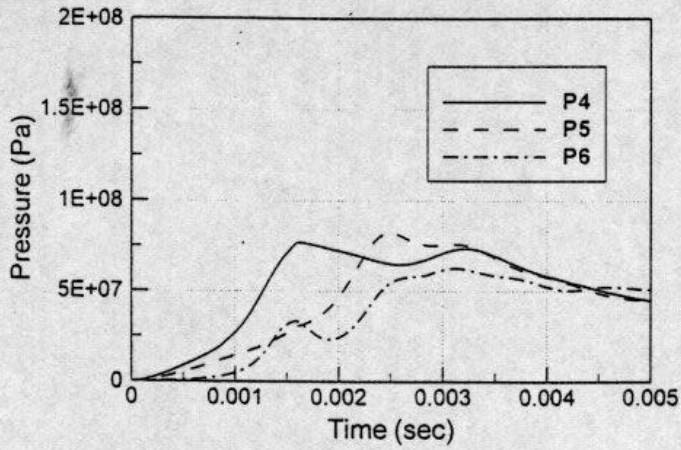


Figure 9. Pressure pulses at node 20, 22, 24 ( $A=0.4 \text{ m}^2$ , Trigger=1 sec)

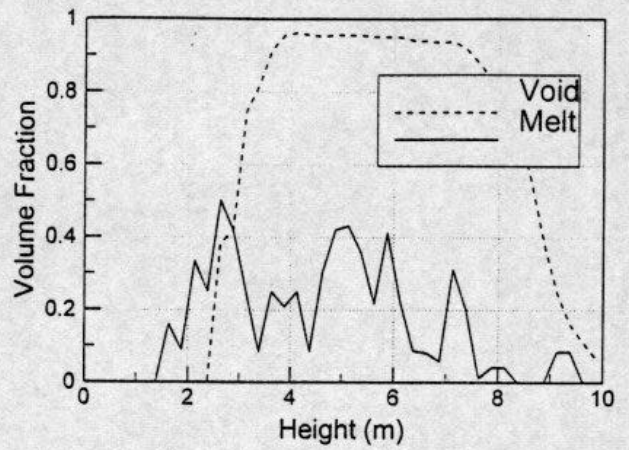


Figure 10. Melt fraction and void fraction in water/gas mixture ( $A=0.2 \text{ m}^2$ , Trigger=2 sec)